Dual Fluorescence from N^6,N^6-Dimethyladenosine

Bo Albinsson

Contribution from the Department of Physical Chemistry, Chalmers University of Technology, S-412 96 Göteborg, Sweden

Received February 18, 1997[⊗]

Abstract: The adenosine derivative N^6,N^6-dimethyladenosine (DMA) shows dual fluorescence in solvents of different polarity. In addition to the "normal" fluorescence at 330 nm, another band is observed at 500 nm. The long wavelength emission dominates in aprotic solvents but is dynamically quenched by protic solvents. Steady-state and lifetime measurements show that the emissions originate from two excited state species; the short wavelength emission is from the directly populated excited state which irreversibly isomerizes into the species responsible for the long wavelength emission. It is conceivable to assign the long wavelength emitting species to a twisted intramolecular charge transfer state (TICT). The fluorescence quantum yield of the short wavelength emission is approximately 4×10^{-4} at room temperature and increases by three orders of magnitude when the temperature is lowered to 80 K in accordance with the behavior of normal nucleic acid bases. In contrast, the long wavelength fluorescence quantum yield is almost temperature independent. The different photophysical processes for DMA are summarized into a kinetic scheme where the temperature quenching of the short wavelength fluorescence is exclusively through isomerization into the long wavelength emitting species. Direct internal conversion to the ground state, commonly believed to be the dominant process for nonradiative deactivation of the DNA bases, makes a negligible contribution for DMA.

Introduction

Excited state lifetimes of the normal nucleic acid bases are very short at room temperature, which has been attributed to an extremely rapid internal conversion.[1−4] This makes the bases and the polynucleotides almost non-fluorescent with fluorescence quantum yields of 10^{-4} or less.[2] The photophysical properties of the nucleic acid bases are important for a mechanistic understanding of the DNA photochemistry. Yet, no mechanism for the suggested rapid internal conversion has been experimentally verified. The prevailing explanation is the near degeneracy of the lowest $^1n\pi^*$ and $^1\pi\pi^*$ states that can lead to an enhancement of the nonradiative decay through vibronic interaction between the states.[5−7]

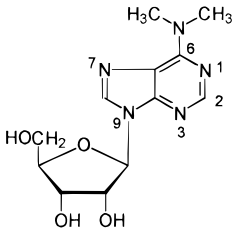

This paper is concerned with the photophysics of the adenosine derivative, N^6,N^6-dimethyladenosine (DMA). Methylation at the exocyclic amino group of adenosine causes a small red shift of the absorption spectrum, but the spectroscopical properties are otherwise similar.[8] The lowest absorption band of adenine at 260 nm derives most of its intensity from two close lying $\pi \rightarrow \pi^*$ transitions.[9−11] Quantum mechanical calculations place one or more $^1n\pi^*$ states in the same energy region as the lowest $^1\pi\pi^*$ state.[12] No direct experimental observation of a low-lying $n\pi^*$ state in adenine has been presented,[13] but comparison with other purine derivatives makes its presence hidden under the main 260-nm band very plausible.[14] For example, from polarized absorption experiments purine was shown to have an $n\pi^*$ state as its lowest singlet state,[15,16] and the second excited singlet state of 2-aminopurine has also been identified as an $n\pi^*$ state.[17,18] The photophysical properties of purine and 2-aminopurine are understood by classical state rules;[19] purine has a phosphorescence quantum yield close to 1 in rigid organic glass, and 2-aminopurine has a high fluorescence quantum yield as expected for molecules with $^1n\pi^*$ and $^1\pi\pi^*$ states as their lowest singlet excited states, respectively. Adenine, for which the lowest $^1n\pi^*$ and $^1\pi\pi^*$ states are predicted to be nearly degenerate, shows weak fluorescence and weak phosphorescence at 80 K.[1,20]

[⊗] Abstract published in *Advance ACS Abstracts,* July 1, 1997.

(1) Eisinger, J.; Lamola, A. A. In *Excited States of Proteins and Nucleic Acids*; Steiner, R. F., Weinryb, I., Eds; Macmillan: New York, 1971; pp 107−198.
(2) Callis, P. R. *Annu. Rev. Phys. Chem.* **1983**, *34*, 329−357.
(3) Cadet, J.; Vigny, P. In *Bioorganic Photochemistry*; Morrison, H., Ed.; John Wiley & Sons: New York, 1990; Vol. 1, pp 1−272.
(4) Ruzsicska, B. P.; Lemaire, D. G. E. In *CRC Handbook of Organic Photochemistry and Photobiology*; Horspool, W. M., Song, P. -S., Eds.; CRC Press: Boca Raton, FL, 1995; pp 1289−1317.
(5) Lim, E. C. *J. Phys. Chem.* **1986**, *90*, 6770−6777.
(6) Madej, S. L.; Okajima, S.; Lim, E. C. *J. Chem. Phys.* **1976**, *65*, 1219−1220.
(7) Lai, T.; Lim, E. C. *Chem. Phys. Lett.* **1979**, *62*, 507−510.
(8) Clark, L. B. *J. Phys. Chem.* **1990**, *94*, 2873−2879.
(9) Clark, L. B. *J. Phys. Chem.* **1995**, *99*, 4466−4470.
(10) Matsouka, Y.; Nordén, B. *J. Phys. Chem.* **1982**, *86*, 1378−1386.
(11) Holmén, A.; Nordén, B.; Broo, A.; Albinsson, B. Unpublished results.
(12) Sreerama, N.; Woody, W.; Callis, P. R. *J. Phys. Chem.* **1994**, *98*, 10397−10407 and references therein.
(13) Phosphorescence excitation spectra on polycrystalline adenosine contained features that were suggested to be due to low-lying $n \rightarrow \pi^*$ transitions: Daniels, M.; Ballini, J. P.; Gräslund, A.; Rupprecht, A.; Åsbrink, L. *Biophys. Chem.* **1988**, *30*, 225−236.
(14) Börresen, H. C. *Acta Chem. Scand.* **1963**, *17*, 921−929.
(15) (a) Clark, L. B.; Tinoco, I., Jr. *J. Am. Chem. Soc.* **1965**, *87*, 11−15. (b) Chen, H. H.; Clark, L. B. *J. Chem. Phys.* **1969**, *51*, 1862−1871.
(16) Albinsson, B.; Nordén, B. *J. Am. Chem. Soc.* **1993**, *115*, 223−231.
(17) Holmén, A.; Nordén, B.; Albinsson, B. *J. Am. Chem. Soc.* **1997**, *119*, 3114−3121.
(18) Smagowicz, J.; Wierrzchowski, K. L. *J. Luminesc.* **1974**, *8*, 210−232.
(19) Turro, N. J. *Modern Molecular Photochemistry*; The Benjamin Cummings Publishers: Menlo Park, CA, 1978; Chapter 5.
(20) Longworth, J. W.; Rahn, R. O.; Shulman, R. G. *J. Chem. Phys.* **1966**, *45*, 2930−2939.

S0002-7863(97)00520-9 CCC: $14.00

Complex fluorescence has been reported from nucleic acid bases in a number of cases. Either multiple emission bands or multicomponent lifetimes[21−24] were observed. Dinucleotides and polynucleotides show exciplex and/or excimer fluorescence from stacked nucleobase structures; in addition to the monomer fluorescence around 300−330 nm, a longer wavelength emission was observed.[25−27] Other sources for fluorescence heterogeneity are the existence of minor tautomeric forms[28] and protonated species.[29] From energetic considerations the only likely tautomeric species for adenine in the ground state involves the 7H−9H prototropic tautomers,[30] and this possibility is ruled out by investigating the 9-methylated derivative or the corresponding nucleoside. Still Ballini et al. observed three components in the time-resolved emission spectra of adenosine and two components for DMA.[31] All three components for adenosine were found to have different excitation spectra and were therefore assigned to different ground-state species, *viz*. two rotational conformers of the exocyclic amino group and one minor protonated species. The relative contributions from the three components were not given, although the short-lived component with fluorescence at short wavelength dominated.

This paper intends to show that in addition to the normal adenine-like fluorescence, DMA has a second long wavelength emission that is associated with a conformationally distorted species formed in an excited state reaction. Twisting of the exocyclic dimethylamino group and partial charge transfer from the dimethylamino group to the purine moiety is the most likely process for forming the conformationally distorted species. It is also suggested that conformational isomerization in the excited state is a possible mechanism for the very efficient radiationless deactivation of this DNA base derivative.

Materials and Methods

Chemicals. N^6,N^6-Dimethyladenosine (DMA) was purchased from Sigma and used without further purification. Aqueous solutions were prepared from deionized water (Millipore), and all organic solvents were of spectrophotometric grade [acetonitrile (ACN) and 1,4-dioxane (dioxane) from Merck and dimethyl sulfoxide (DMSO) from Jansen]. 2-Methyltetrahydrofuran (2MTHF) from ACROS contained hydroxytoluene (1%) as a stabilizer, which was removed by fractionated distillation immediately before use. All solvents were checked for background emission.

Absorption and Emission Measurements. Absorption spectra were measured with a CARY 4B UV/vis spectrometer. Steady-state emission measurements were performed on a SPEX fluorolog $\tau 2$ spectrofluorimeter. Quantum yields of fluorescence (ϕ_f) were determined relative to the quantum yield of an argon purged solution of 2,5-diphenyloxazole (PPO) in cyclohexane ($\phi_f = 0.85$).[32] The measurements were performed on optically matched samples (same absorbance at the wavelength of excitation), and the quantum yields are corrected for differences in refractive index. The fluorescence excitation spectra were measured on samples with maximum absorbance less than 0.1 in order to avoid inner filter distortion. Low-temperature measurements were done in a temperature-controlled liquid N_2 cryostat (Oxford Instruments DN 1704 with temperature controller DTC2). Phosphorescence lifetimes were measured by manually closing the excitation shutter while recording the emission intensity (response time of about 0.1 s). The fluorescence lifetimes were measured by time-correlated single-photon counting, using a nitrogen filled flash lamp (Oxford instruments) as the excitation source.[33] A diluted silica sol scattering solution was used as a reference. The fluorescence decays were analyzed by convolution of the excitation pulse and multiexponential fitting of the fluorescence decay with the Globals software.[34] This setup has an estimated time resolution of better than 100 ps.

Results

The material is organized as follows. (i) Room temperature fluorescence measurements of DMA in aprotic solvents show two distinct peaks; the "normal" short wavelength (B-state)[35] fluorescence at about 30 000 cm^{-1} (330 nm) from the directly populated excited state and the long wavelength (A-state)[35] fluorescence at about 20 000 cm^{-1} (500 nm). (ii) The A-state fluorescence is quenched by protic solvents and its peak wavelength is solvent sensitive. The quenching is dynamic with a near diffusion controlled rate. (iii) The B-state fluorescence quantum yield is strongly dependent on temperature and increases 1000-fold between room temperature and 80 K. DMA also shows phosphorescence in vitrified organic glass with a quantum yield similar to the fluorescence quantum yield. In contrast, the A-state fluorescence is almost independent of temperature. (iv) The time-resolved fluorescence of DMA is analyzed globally as a function of emission wavelength and supports the mother−daughter relation between the B- and A-states. (v) The observations are summarized in a kinetic scheme where the relative importance of the different nonradiative deactivation channels (triplet formation, direct internal conversion, and isomerization to the A-state) are discussed.

(i) Dual Fluorescence from DMA in Different Solvents. Figure 1 shows the absorption and fluorescence emission spectra of DMA in H_2O, ethanol, ACN, and dioxane. The absorption spectra are very similar in the different solvents and the peak wavenumber for the lowest electronic absorption band is 36 300 cm^{-1}. The emission spectrum shows two peaks: one at around 30 000 cm^{-1} (B-fluorescence) and one at lower energy around 20 000 cm^{-1} (A-fluorescence). In contrast to the absorption both the A- and B-fluorescence are sensitive to change in solvent polarity. The fluorescence characteristics are summarized in Table 1, where it is clearly seen that the emissions are red shifted in polar compared to less polar solvents. In addition, the fluorescence quantum yield for the A-fluorescence but not for the B-fluorescence depends strongly on solvent. The A-fluorescence quantum yield is a factor of 10 smaller in the protic solvents (Table 1). The shape of the emission spectrum in all different solvents is independent of the excitation wavelength, and the shape of the excitation spectrum is superimposable on the absorption spectrum and is, likewise, independent of the emission wavelength. The shapes of the emission spectra in general and the relative quantum yields of the A- and B-fluorescence in particular are independent of the

(21) Ballini, J. P.; Vigny, P.; Daniels, M. *Biophys. Chem.* **1983**, *18*, 61−65.
(22) Ballini, J. P.; Daniels, M.; Vigny, P. *Eur. Biophys. J.* **1988**, *16*, 131−142.
(23) Riegler, R.; Claesens, F.; Kristensen, O. *Anal. Instrum.* **1985**, *14*, 525−546.
(24) Georghiou, S.; Nordlund, T. M.; Saim, A. M. *Photochem. Photobiol.* **1985**, *41*, 209−212.
(25) Vigny, P.; Favre, A. *Photochem. Photobiol.* **1974**, *20*, 345−349.
(26) Vigny, P.; Duquesne, M. in *Organic Molecular Photophysics*; Birks, J. B., Ed.; Wiley: New York, 1976; pp 167−177.
(27) Vigny, P.; Ballini, J. P. In *Excited States in Organic Chemistry and Biochemistry*; Pullman, B., Goldblum, N., Eds.; Reidel: Dodrecht, Holland, 1977; pp 1−13.
(28) Wilson, R W.; Callis, P. R. *Photochem. Photobiol.* **1980**, *31*, 323−327.
(29) Kononov, A. I.; Bakulev, V. M. *J. Photochem. Photobiol. B: Biol.* **1996**, *34*, 211−216.
(30) Holmén, A.; Broo, A. *Int. J. Quantum Chem.: Biol. Symp.* **1995**, *22*, 113−122 and references therein.
(31) Ballini, J. P.; Daniels, M.; Vigny, P. *Eur. Biophys. J.* **1988**, *16*, 131−142.
(32) Takahashi, T.; Kikuchi, K.; Kokubun, H. *J. Photochem.* **1980**, *14*, 67−70.
(33) This setup is described in detail in the following: Löfroth, J. E. Ph. D. Thesis, University of Göteborg, 1982.
(34) Globals Unlimited, Revision 3: Beechem, J. M.; Gratton, E.; Mantulin, W. W., The Laboratory of Fluorescence Dynamics: University of Illinois at Urbana−Champaign, 1992.
(35) The labels A and B are, at this point, introduced to simplify notation.

Table 1. Fluorescence Characteristics for DMA at Room Temperature (293 K)

solvent	ϵ_r[a]	n_D[a]	$\bar{\nu}_{abs}$/cm^{-1}	$\bar{\nu}_{FB}$/cm^{-1}	$\bar{\nu}_{FA}$/cm^{-1}	Φ_{FB}	Φ_{FA}	τ_{FA}/ns
H_2O	80.4	1.333	36 300	28 180	17 600	3.5×10^{-4}	2.6×10^{-4}	*b*
D_2O	80.4	1.333	36 300	28 180	17 600	4×10^{-4} [c]	3.4×10^{-4}	*b*
DMSO	47.2	1.478	36 300	29 670	20 160	6.5×10^{-4}	4.6×10^{-3}	*b*
ethanol	25.3	1.361	36 300	29 390	18 800	3.5×10^{-4}	4.7×10^{-4}	*b*
ACN	37.5	1.342	36 300	29 085	19 400	4.2×10^{-4}	2.7×10^{-3}	0.71
2MTHF	6.97	1.406	36 300	30 140	20 400	4.8×10^{-4}	5.2×10^{-3}	1.15
dioxane	2.22	1.422	36 300	30 060	20 300	5.1×10^{-4}	6.2×10^{-3}	1.27

[a] Reference 52. [b] Not determined. [c] Uncertain due to high background emission.

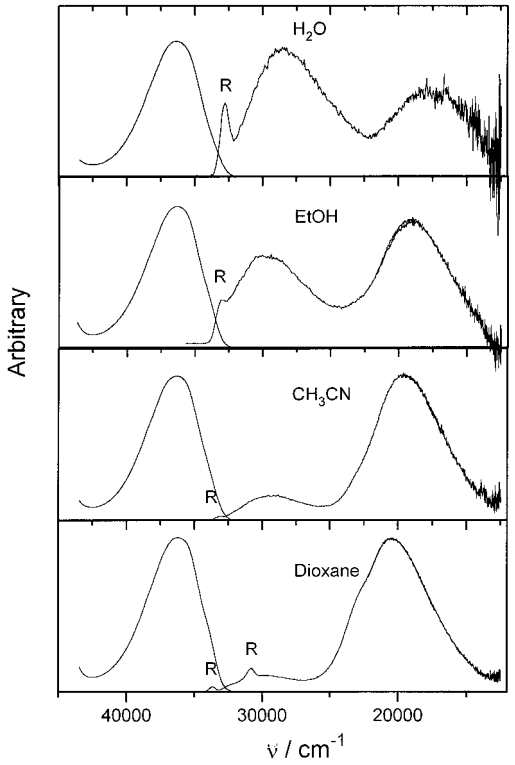

Figure 1. Fluorescence (right curve) and absorption (left curve) spectra of DMA in H_2O, ethanol, ACN, and dioxane. The fluorescence was excited at 36 400 cm^{-1} for H_2O, ethanol, and ACN solutions and at 33 900 cm^{-1} for the dioxane solution. Unavoidable Raman and Rayleigh scattering peaks from the solvent are labeled R.

solute concentration (10^{-3}−10^{-6} M). These results indicate that the A-fluorescence originates from an excited state reaction which is independent of solute concentration and that the A-state is formed in solvents of different polarity. The excited precursor to the A-state is presumably the directly excited B-state and the B to A conversion is likely to be an intramolecular process.

(ii) The A-State Fluorescence Is Quenched by Protic Solvents. The quantum yield of the A-fluorescence is significantly smaller in the protic solvents than in aprotic solvents as seen in Table 1. In Figure 2 the fluorescence spectra of DMA in pure dioxane and in dioxane/H_2O mixtures are shown. Upon addition of H_2O the intensity of the A-fluorescence decreases while the intensity of the B-fluorescence remains constant. No significant effects were detected on the absorption spectra of the same samples. The lifetime of the A-fluorescence decreases in parallel to the intensity showing that the A-state is dynamically quenched by H_2O. A similar behavior was found when adding methanol to DMA in dioxane. These measurements suggest that the protic solvents primarily quench the A-state but influence the B- to A-state conversion only marginally. The quantum yield of the B-fluorescence is independent of quencher concentration (Figure 2), which shows that the B- to A-state conversion is irreversible.

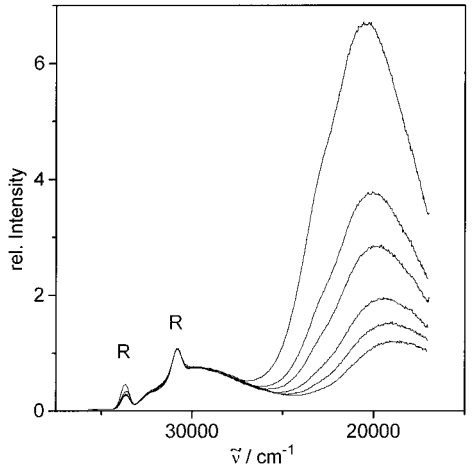

Figure 2. Fluorescence quenching of DMA in dioxane by H_2O. The concentrations of H_2O are (from top to bottom) 0, 0.42, 0.88, 2.22, 4.75, and 9.76 M. Unavoidable Raman and Rayleigh scattering peaks from the solvent are labeled R.

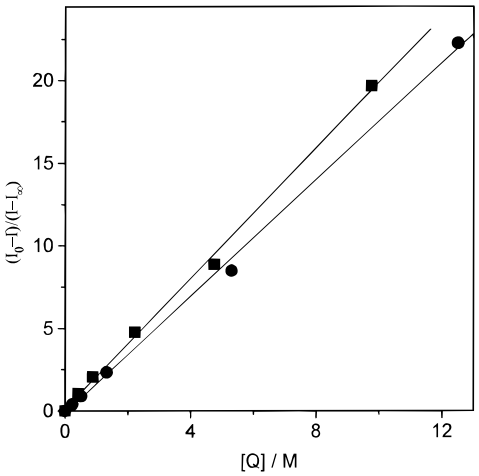

Figure 3. Modified Stern−Volmer plot of DMA in dioxane quenched by H_2O (●) and methanol (■).

The quenching of the DMA A-fluorescence with protic solvents follows normal Stern−Volmer[36] behavior at low quencher concentration, i.e. the inverse of the fluorescence intensity and lifetime increase linearly with quencher concentration. However, at high quencher concentration significant negative deviation from a straight line is noted. Even in pure water and methanol DMA shows A-fluorescence, albeit much weaker. In Figure 3 a modified Stern−Volmer plot[37] is shown

(36) $I_0/I = \tau_0/\tau = 1 + K[Q] = 1 + k_q\tau_0[Q]$, where I (τ) and I_0 (τ_0) are the intensities (lifetimes) at quencher concentrations [Q] and [Q] = 0, respectively. For a derivation of the Stern−Volmer equation see ref 38.

(37) For samples where the quenched species show residual fluorescence the measured intensities (I) are related to the quencher concentration ([Q]) by $(I_0 - I)/(I - I_\infty) = K[Q]$, where I_0 and I_∞ are the fluorescence intensities in pure solvent and in pure quencher, respectively, and K is the normal Stern−Volmer constant.

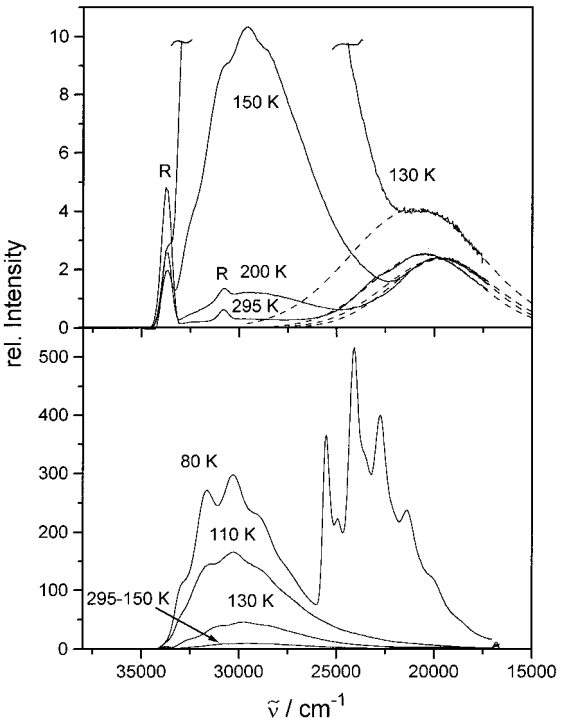

Figure 4. Temperature dependence of the DMA emission in 2MTHF (295−80 K). The top panel shows spectra at temperatures above 130 K on a magnified scale. The dashed lines show Gaussian fits to the A-fluorescence bands (see text). Unavoidable Raman and Rayleigh scattering peaks from the solvent are labeled R.

where the measured intensities are compensated for the residual fluorescence intensities in methanol and H_2O. The Stern-Volmer constant, K, for DMA in dioxane quenched by H_2O and methanol is 2.0 and 1.8 M^{-1}, respectively. Knowledge of the A-fluorescence lifetime in dioxane (Table 1) allows calculation of the corresponding bimolecular quenching constants, k_q. They are found to be 1.6×10^9 and 1.4×10^9 M^{-1} s^{-1} for H_2O and methanol quenching, respectively. This shows that the quenching of the A-fluorescence is nearly diffusion controlled.

Undoubtedly the A-state energy, as measured by the spectral position of the fluorescence maximum, is sensitive to solvent polarity. Table 1 shows the spectral positions of the fluorescence maxima for the A- and B-fluorescence. Both the A- and B-fluorescence are red shifted with increasing solvent polarity, indicating a larger dipole moment in the respective excited states compared to the ground state. The red shift is slightly larger for the A-fluorescence.

(iii) Temperature Dependence of the A- and B-Fluorescence. The fluorescence quantum yields for DMA at room temperature are very small, of the order 4×10^{-4} for the B-fluorescence and 5×10^{-3} for the unquenched A-fluorescence (Table 1). This is a common feature of all the normal nucleic acid bases, for which the quantum yields at room temperature are between 5×10^{-5} and 1×10^{-4}. Figure 4 shows the fluorescence emission of DMA in 2MTHF at different temperatures between 295 and 80 K. The upper panel shows the high-temperature spectra (295−130 K) on a magnified scale. In order to resolve the A- and B-fluorescence contributions to the observed emission spectra, the former was fitted to a Gaussian band shape (dashed line in the upper panel of Figure 4). At room temperature the A-state fluorescence is about 10 times stronger than the B-fluorescence, at 200 K they are of similar magnitude, and at lower temperatures the B-fluorescence dominates. The B-fluorescence, thus, depends strongly on temperature and increases 1000-fold between 295 and 80 K.

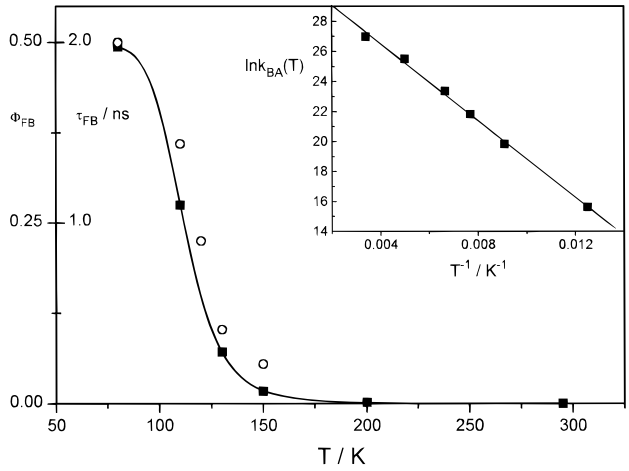

Figure 5. Temperature dependence of the quantum yield (■) and lifetime (○) of the B-fluorescence. The Arrhenius plot of the B → A isomerization rate constant vs inverse temperature is shown in the insert.

At 80 K, where 2MTHF forms a solid glass, phosphorescence of similar magnitude as the B-fluorescence is also observed.

The strong temperature dependence of the B-fluorescence is contrasted by the very weak dependence shown by the A-fluorescence (Figure 4). The quantum yield of the A-fluorescence is essentially constant between 295 and 150 K. It increases slightly at 130 K, and at lower temperatures it is impossible to resolve due to its weakness in comparison to the B-fluorescence.

A similar temperature dependence was observed for the emission from DMA in a 9:1 ethanol/methanol mixture which forms a stable glass at 110 K (not shown). There, however, the intrinsic temperature dependence of the A-fluorescence is obscured by changes in diffusion-controlled quenching by the solvent and, thus, a larger temperature effect than in 2MTHF was observed.

Figure 5 shows the temperature dependence of the B-fluorescence quantum yield in 2MTHF. The B-fluorescence lifetime is also plotted for temperatures below 150 K. Figure 5 also shows inserted the temperature dependence of the B-fluorescence analyzed as a simple one pathway Arrhenius activated radiationless deactivation. This will be discussed together with the suggested kinetic model below.

(iv) Fluorescence Lifetimes. The lifetime of the B-fluorescence of DMA at 80 K in 2MTHF is 2.0 ns. It decreases in parallel to the fluorescence quantum yield when the temperature is changed between 80 and 150 K, showing that the radiative rate constant k_{FB} is independent of temperature. The lifetime at room temperature estimated from the changes in the fluorescence quantum yield is $\tau_{FB}(293\ K) \approx 2$ ps, i.e. too short to be accurately resolved by our equipment. The A-fluorescence on the other hand is fairly long-lived at room temperature, e.g. $\tau_{FA} = 1.15$ ns in 2MTHF (Table 1). Table 2 summarizes an attempt to globally analyze the fluorescence decay as a function of wavelength for DMA in ACN at room temperature. Two components with varying contributions at different wavelengths are identified: one short lived associated with the B-fluorescence and one with a longer lifetime associated with the A-fluorescence. As expected, the short-lived component dominates the decay at short wavelengths and the long-lived component dominates at long wavelengths. In addition, it is seen in Table 2 that the short-lived component has a negative preexponential factor for long-wavelength emission as expected for an excited state reaction B → A. A similar behavior was found for DMA in 2MTHF at 150 K and for DMA in dioxane at 290 K.

Table 2. Fluorescence Lifetimes of DMA in ACN at 293 K[a]

	λ_{em}/nm					
	360	420	460	500	540	580
α_1	6.5	1.74	0.67	0.33	−0.17	−0.26
τ_1/ns			0.05 ± 0.05[c]			
f_1[b]	0.44	0.17	0.10	0.08	0.04	0.06
α_2	0.69	1.00	1.26	1.50	1.03	1.63
τ_2/ns			0.71 ± 0.01			
f_2[b]	0.56	0.83	0.90	0.92	0.96	0.94

[a] The emission decays were fitted globally to a biexponential expression: $I(t,\lambda) = \alpha_1(\lambda)\exp(-t/\tau_1) + \alpha_2(\lambda)\exp(-t/\tau_2)$ where the two lifetimes (τ_1 and τ_2) were linked and the preexponential factors (α_1 and α_2) varied freely. [b] Fractional intensities calculated for an irreversible excited state reaction, 1 → 2: $f_1(\lambda) = \tau_2^{-1}[(\alpha_1(\lambda) + \alpha_2(\lambda))/(\alpha_1(\lambda)\tau_2^{-1} + \alpha_2(\lambda)\tau_1^{-1})]$ and $f_2(\lambda) = [(\alpha_2(\lambda)(\tau_1^{-1} - \tau_2^{-1}))/(\alpha_1(\lambda)\tau_2^{-1} + \alpha_2(\lambda)\tau_1^{-1})]$. [c] The short lifetime is inaccurate due to instrumental limitations.

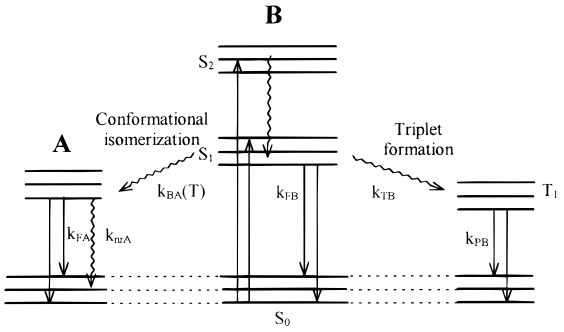

Figure 6. Proposed photophysical model for DMA. Values of the five temperature independent rate constants and Arrhenius parameters for the temperature dependent B → A isomerization reaction are given in the text.

(v) Kinetic Model. The observed photophysical behavior of DMA is summarized by the energy level diagram in Figure 6. After excitation to the B-state three competing deactivation processes of the B-state are considered: direct fluorescence (k_{FB}), triplet formation (k_{TB}), and conformational isomerization into the A-state (k_{BA}). It will be shown below that all present observations are consistent with this kinetic scheme where the B- to A-state conversion is the only temperature-dependent process.

At 80 K in 2MTHF glass the quantum yields of B-state phosphorescence and fluorescence are $\Phi_{PB} = \Phi_{FB} = 0.5$. The fluorescence and phosphorescence lifetimes are $\tau_{FB} = 2.0$ ns and $\tau_{PB} = 5.2$ s, which give the radiative rate constants for fluorescence and phosphorescence from the B-state $k_{FB} = 2.5 \times 10^8$ s^{-1} and $k_{PB} = 0.19$ s^{-1} (Figure 6). The fluorescence and phosphorescence quantum yields add up to unity, showing that direct nonradiative return to the ground state is negligible at 80 K. Consequently, at this temperature triplet formation is the only process that competes with fluorescence from the B-state and $k_{TB} = \tau_{FB}^{-1} - k_{FB} = 2.5 \times 10^8$ s^{-1} (Figure 6).

At higher temperatures the fluorescence from the B-state is quenched by an additional deactivation mechanism: the B to A state conversion. With the proposed kinetic scheme the fluorescence quantum yield of the B-state is given by

$$\Phi_{FB} = \frac{k_{FB}}{k_{FB} + k_{TB} + k_{BA}(T)}$$

Rearranging this equation, assuming k_{FB} and k_{TB} to be independent of temperature, and assuming $k_{BA}(T)$ to have an Arrhenius type temperature dependence yields

$$\ln k_{BA}(T) = \ln A - \frac{E_a}{RT} = \ln\left\{\left(\frac{1}{\Phi_{FB}} - 1 - \frac{k_{TB}}{k_{FB}}\right)k_{TB}\right\}$$

where E_a is the activation energy and A is the preexponential factor for the B → A process. A plot of $\ln k_{BA}(T)$ vs $1/T$ yields the straight line inserted in Figure 5 with $A = 5.4 \times 10^{13}$ s^{-1} and $E_a = 2.5$ kcal/mol.

Since the B → A process is irreversible (*vide supra*) the observed fluorescence quantum yield of the A-state (Φ_{FA}) is simply the intrinsic quantum yield (Φ_A^{int}) times the quantum yield for A-state formation (Φ_{BA})

$$\Phi_{FA} = \Phi_A^{int}\Phi_{BA} = \frac{k_{FA}}{(k_{FA} + k_{nrA})}\frac{k_{BA}(T)}{(k_{FB} + k_{TB} + k_{BA}(T))}$$

At T ≥ 130 K the deactivation of the B-state is dominated by isomerization to the A-state and, consequently, $\Phi_{BA} \approx 1$. The observed quantum yield for A-fluorescence is essentially temperature independent (Figure 4) in spite of the greatly varying rate for A-state formation. This is consistent with the proposed kinetic model because at temperatures where the A-fluorescence is observed ($T \geq 130$ K) the formation is almost quantitative ($\Phi_{BA} \approx 1$) and the intrinsic quantum yield (Φ_A^{int}) varies only slightly with temperature. The rate constants for fluorescence (k_{FA}) and nonradiative deactivation (k_{nrA}) of the A-state are found from measurements of the lifetime and quantum yield of the A-fluorescence. At room temperature in 2MTHF we find $\Phi_{FA} = 5.2 \times 10^{-3}$ and $\tau_{FA} = 1.15$ ns (Table 1), which gives $k_{FA} = 4.5 \times 10^6$ s^{-1} and $k_{nrA} = 8.7 \times 10^8$ s^{-1}.

Discussion

The A-Fluorescence Is Due to an Excited State Reaction. When two emission bands are observed from a sample it is either due to two different ground state species or one single species that undergoes a photophysical or photochemical transformation, i.e. an excited state reaction.[38] In the case of DMA, since the fluorescence quantum yield is very small at room temperature, the possibility to detect emission from either minor impurities or a less stable ground state species related to DMA has to be considered. The A-fluorescence, being the unusual fluorescence from DMA, is separated from the absorption by more than 15 000 cm^{-1}. If an impurity or a different ground state species were responsible for the A-fluorescence one would expect its excitation spectrum to be different from the excitation spectrum of the B-fluorescence. Since the A- and B-fluorescence bands are so well separated, the corresponding absorption spectra of these two (hypothetical) ground state species would also be well separated and it should have been possible to excite the A-fluorescence at wavenumbers well below the normal absorption spectrum of DMA. In reality the excitation spectra match exactly, and they also match the absorption spectrum within experimental limitations. No A-fluorescence at all is observed for excitation wavenumbers below 30 000 cm^{-1}, not even in concentrated solutions. Of course two different ground state species might have exactly the same absorption spectra, but in that case one of these species has a world-record Stokes shift of at least 15 000 cm^{-1}. We consider this possibility as less likely.

The A- and B-fluorescence have different lifetimes with $\tau_{FA} = 1.15$ ns and $\tau_{FB} < 100$ ps for DMA in room temperature 2MTHF (Table 2). The quick decay of the B-state is detected as a risetime of the A-fluorescence, i.e. with a negative preexponential factor, when the time-resolved fluorescence as

(38) Lakowicz, J. R. *Principles of Fluorescence Spectroscopy*; Plenum Press: New York, 1983.

a function of wavelength is analyzed globally. This is another indication for an excited state reaction rather than heterogeneity in the ground state, which also would yield two lifetimes but with positive preexponential factors at all wavelengths. The decay times deduced from the analysis are associated with the intrinsic decays of the A- and B-states since the excited state reaction is found to be irreversible.

The Excited State Reaction is Intramolecular. DMA does not seem to decompose and no new features in the absorption or emission spectra have been detected after hours of illumination in the spectrofluorimeter. It is therefore not expected that the excited state reaction produces a new stable chemical species. The intensity of the A-fluorescence does not depend on solute concentration in the range $10^{-3}-10^{-6}$ M, why it is unlikely that bimolecular complexes in the ground state or complexes formed in the excited state (exciplex or excimer) are responsible for the A-fluorescence. The latter is also unlikely due to the very short lifetime of the precursor B-state at room temperature. In summary it is concluded that the A-fluorescence is due to an *intramolecular excited state reaction*, but no ground state species related to the A-state has been observed. The reaction is irreversible in the excited state, at least at the conditions used in the quenching experiments (Figure 2).

Twisted Intramolecular Charge Transfer—TICT? It is important to find out the nature of the observed intramolecular excited state reaction for DMA, in particular since the A-state is long lived in comparison with the directly excited B-state and might be a potential precursor state for photochemistry. Also since the temperature quenching of the primary excited state (B-state) is proposed to occur via the A-state, its properties need to be thoroughly investigated.

Since the first observation by Lippert[39] of dual fluorescence from 4-(dimethylamino)benzonitrile (DMABN) and the assignment proposed by Grabowski and co-workers[40] that the unusual long wavelength fluorescence was due to a charge transfer from the dialkylamino group to the benzonitrile moiety followed by twisting of the dimethylamino group, a number of molecules have been suggested to have this so-called TICT emission.[41,42] One characteristic feature of the TICT emission is its sensitivity toward solvent polarity: for DMABN the emission maximum red shifts and the rate of TICT state formation increases with increasing solvent polarity. In addition it is found for many heteroaromatic molecules in general, and the TICT molecules in particular, that the fluorescence is quenched by protic solvents.

The dual fluorescence from 4-(dialkylamino)pyrimidines has been accounted for by the TICT mechanism.[43−46] 4-(Dimethylamino)pyrimidine and DMA are structurally related, sharing the pyrimidine core. For the 4-(dialkylamino)pyrimidines it was found that ortho substitution increased the rate of TICT state formation, and this has been explained by the larger ground state twist of the *N*,*N*-dimethylamino group (pretwist).[43] In DMA the imidazole part acts sterically as an ortho substituent and, thus, the dimethylamino group of DMA is likely to be somewhat twisted in the ground state. A number of characteristic features found for the TICT emission agree with the present observation of the A-fluorescence. It is therefore tempting to assign the A-state of DMA to be a TICT state. However, the A-fluorescence quantum yield of DMA is largest in the least polar solvents, and the emission maxima for the B- and A-fluorescence are both red shifted almost equally by increased solvent polarity. These observations are not fully in accordance with the normal TICT model, and further investigation of solvent effects on N^6,N^6-dimethyl-9-ethyladenine complemented by quantum mechanical calculations are underway in order to resolve this issue.[47]

Adenosine Decays Nonradiatively through the A-State? In the suggested kinetic scheme (Figure 6) the quenching of the B-state at temperatures above 130 K is dominated by isomerization into the A-state followed by a nanosecond decay. However, the prevailing view of the adenosine (and other nucleosides) photophysics is that the ground state is recovered within picoseconds.[1−4,48,49] If this is true for DMA a direct return from the B-state to the ground state *competing* with the A-state formation has to be included in the kinetic scheme and just a small portion of the molecules primarily excited into the B-state converts to the A-state. In that case since the lifetime of the B-state is estimated to be only a few picoseconds, the A-state formation has to have a rate constant of at least 10^9 s^{-1} at room temperature in order to yield the observed A-fluorescence quantum yield. This is an acceptable model if only the room temperature measurements were at hand. Now, the fluorescence quantum yield and lifetime of the B-state increase as the temperature is lowered, i.e. the rate for the anticipated competing direct internal conversion decreases. To have both simple one-exponential Arrhenius behavior of the B-fluorescence quantum yield (Figure 5) and a constant A-fluorescence quantum yield would require the A-state formation to have the same temperature dependence as the anticipated direct internal conversion, i.e. the same activation energy. Otherwise, an increased A-fluorescence at lower temperatures would have resulted. This coincidence that the A-state formation is thermally activated with the same activation energy as the radiationless decay of the B-state led us to believe the two processes were coupled, i.e. they are one and the same process.

The kinetic scheme proposed in Figure 6 is the simplest possible that explains the different emissions and their temperature dependence. Of course it is possible to suggest a more complex scheme and future measurements might require that. The rate constants concluded for DMA in 2MTHF are all of reasonable size. The radiative rate constant, k_{FB}, for fluorescence from the B-state is related to the size of the transition dipole moment of the $S_0 \rightarrow S_1$ transition, and its value, 1.1×10^{-29} Cm = 3.2 D, is reasonable for an allowed $\pi \rightarrow \pi^*$ transition.[50] The radiative rate constant for the B-state phosphorescence, k_{PB}, is related to the $S_0 \rightarrow T_1$ transition. The phosphorescence from purine derivatives has been shown to originate from a $^3(\pi\pi^*)$ state[1,16] and the very small rate constant for phosphorescence reflects the very low transition probability.

(39) Lippert, E. *Z. Naturforsch.* **1955**, *10A*, 541−545.
(40) Rotkiewicz, K.; Grellmann, K. H.; Grabowski, Z. R. *Chem. Phys. Lett.* **1973**, *19*, 315−318.
(41) Rettig, W. *Angew. Chem., Int. Ed. Engl.* **1986**, *25*, 971−988.
(42) Bhattacharyya, K.; Chowdhury, M. *Chem. Rev.* **1993**, *93*, 507−535.
(43) Herbich, J.; Grabowski, Z. R.; Wójtowicz, H.; Golankiewicz, K. *J. Phys. Chem.* **1989**, *93*, 3439−3444.
(44) Herbich, J.; Salgado, F. P.; Rettschnick, R. P. H.; Grabowski, Z. R.; Wójtowicz, H *J. Phys. Chem.* **1991**, *95*, 3491−3497.
(45) Herbich, J.; Karpiuk, J.; Grabowski, Z. R.; Tamai, N.; Yoshihara, K. *J. Luminesc.* **1992**, *54*, 165−175.
(46) Herbich, J.; Waluk, J. *Chem. Phys.* **1994**, *188*, 247−265.
(47) Holmén, A.; Albinsson, B. Unpublished material.
(48) Nikogosyan, D. N.; Angelov, D.; Soep, D.; Lindqvist, L. *Chem. Phys. Lett.* **1996**, *252*, 322−326.
(49) Oraevsky, A. A.; Sharkov, A. V.; Nikogosyan, D. N. *Chem. Phys. Lett.* **1981**, *83*, 276−280.
(50) The radiative rate constant is approximately related to the transition moment (M_{01}) by the following expression: $k_F = (64\pi^4/3h)(1/4\pi\epsilon_0)\cdot n^3\tilde{\nu}^3_{max}M_{01}^2$, where n is the refractive index of the solvent, ϵ_0 is the permittivity for vacuum, and $\tilde{\nu}_{max}$ is the maximum wavenumber of the fluorescence band. Birks, J. B. *Photophysics of Aromatic Molecules*; Wiley: New York, 1970; p 48.

The radiative rate constant for fluorescence from the A-state is $k_{FA} = 4.5 \times 10^6\ s^{-1}$. This corresponds to a forbidden singlet−singlet transition with a transition moment of 0.8 D in keeping with the observations of TICT fluorescence from other molecules.[41] The forbidden nature of the charge transfer transition involved in the TICT fluorescence has been explained by the small overlap between two orbitals located on different π-systems for the twisted geometry.[41] The nonradiative rate constant for the A-state comprises both internal conversion and intersystem crossing and dominates the decay of the A-state, $k_{nrA} = 8.7 \times 10^8\ s^{-1}$.

Three channels deactivate the directly excited B-state, *viz.* fluorescence, triplet formation, and isomerization into the A-state. The radiative rate constant for fluorescence was shown to be approximately independent of temperature between 80 and 150 K, and since no obvious change in the absorption spectrum with temperature is observed between 80 and 295 K, it is a reasonable assumption that k_{FB} is independent of temperature. Triplet formation is usually not dependent on temperature, but some cases have been reported where the triplet formation is thermally activated due to the near degeneracy of S_1 and T_2.[51] For different purine derivatives it has been argued that the rate constant for triplet formation is essentially independent of temperature.[1] No measurements on DMA have been performed to verify that k_{TB} is constant, but it seems to be a reasonable assumption in comparison with other purines. Furthermore, if the rate of triplet formation increased with increasing temperature it would compete with A-state formation and the same arguments that were used to rule out direct internal conversion should be valid in this case too. Finally, the concluded parameters for the thermally activated A-state formation, $A = 5.4 \times 10^{13}\ s^{-1}$ and $E_a = 2.5$ kcal/mol, seem reasonable for a unimolecular isomerization reaction.

The low fluorescence quantum yield and short lifetime of the primary excited state of DMA is proposed to be due to an excited state reaction into a conformationally distorted species, the A-state, which acts as a bottle-neck for ground state recovery with a nanosecond lifetime. Is this a general mechanism for the radiationless deactivation of other DNA bases and in particular for adenosine? The "common" observable photophysical properties for adenosine and DMA are the temperature dependence of the lifetime and quantum yield of the directly excited states and these are clearly related. However, no unusual long wavelength emission is observed for adenosine under the same conditions where it is observed for DMA. This is either because the A-state is more efficiently quenched in adenosine or no A-state is formed. The latter would require a totally different mechanism for radiationless deactivation in adenosine than in DMA, presumably direct internal conversion, or that the deactivation and conformational isomerization processes are related in a still unknown way. Further research will resolve this important issue.

Conclusions

DMA shows dual fluorescence in a range of solvents. The two emissions were assigned to two different species in the excited state: the B- and A-states. Nonradiative deactivation of DMA was shown to occur exclusively through the A-state at room temperature. The transformation from the B- to the A-state was thermally activated with an Arrhenius activation energy of 2.5 kcal/mol. Charge transfer from the dimethylamino group to the purine ring followed by twisting, the so-called TICT mechanism, was suggested as a likely candidate to account for the A-state.

Acknowledgment. I am grateful to Dr. Kjell Sandros and M. Sc. Anders Holmén for stimulating discussions. This work was supported by the Natural Science Research Council (NFR) of Sweden.

JA9705203

(51) Almgren, M. *Mol. Photochem.* **1972**, *4*, 327−338.
(52) *CRC Handbook of Chemistry and Physics*, 75th ed.; Lide, D. R., Ed.; CRC Press: Boca Raton, FL, 1995.